Available online at www.sciencedirect.com
ScienceDirect
Solar Energy Materials & Solar Cells 91 (2007) 1392–1397
Solar Energy Materials and Solar Cells
www.elsevier.com/locate/solmat

S and Te inter-diffusion in CdTe/CdS hetero junction

J. Pantoja Enríquez[a,*], E. Gómez Barojas[b], R. Silva González[c], U. Pal[c]

[a]*Cuerpo Académico-Energía y Sustentabilidad, Universidad Politécnica de Chiapas, Eduardo J. Selvas S/N, Col. Magisterial, Tuxtla Gutiérrez 29010, Chiapas, Mexico*
[b]*CIDS-ICUAP, Apdo. Postal 1651, 72000 Puebla, México*
[c]*Instituto de Física, Benemérita Universidad Autónoma de Puebla, Puebla, Mexico*

Available online 21 June 2007

Abstract

Effects of post formation thermal annealing of the CdTe–CdS device on the inter-diffusion of S and Te at the junction in a substrate configuration device have been studied by Auger electron spectroscopy. While the migration of S and Te atoms increases with annealing temperature, the extent of S diffusion is always higher than the diffusion of Te atoms. Inter-diffusion of S and Te causes the formation of $CdTe_{1-x}S_x$ ternary compound at the CdTe–CdS interface.

Keywords: CdS; CdTe; AES; CdTe/CdS; Inter-diffusion

1. Introduction

CdTe based photovoltaic devices are highly interesting due to the availability of a variety of CdTe film fabrication techniques such as electrodeposition, sputtering, physical vapor deposition and close spaced sublimation (CSS) [1–5]. A good number of reports and reviews are available on the characterization of both CdTe films [6–13] and CdTe/CdS devices [14–20]. Post fabrication annealing of the CdTe–CdS hetero-structures is a very common practice and critical to improve their photovoltaic performance in fabrication of solar cells. For solar cell fabrication, generally, the CdTe/CdS hetero-structures are annealed in $CdCl_2$ atmosphere in between 350 and 450 °C [21–23], which promotes the recrystallization, grain growth, diffusion of sulfur (S) and tellurium (Te), enhanced p-type conductivity of the CdTe and passivation of defects present at the interface [24,25]. However, the diffusion process depends on the annealing temperature, annealing time, distribution of grains and defect density of the material. The quantification of S and Te inter-diffusion between CdTe and CdS during the post deposition treatment is important in optimizing the annealing process and understanding the devices operation.

The Te diffusion in to the CdS layer produces $CdS_{1-y}Te_y$ ternary compound, with a band gap less than that of the CdS, increasing the light absorption in the window layer thereby diminishing the J_{sc} of the device [24]. In analogous way the diffusion of S in to CdTe forms the compound $CdTe_{1-x}S_x$. The effect of the formation of this compound in the performance of the device is not clear, however, a correlation between spectral response at the absorption edge of CdS and the intermixing of CdTe and CdS has been reported [26]. The intermixing of CdTe and CdS results in a decrease in band gap of CdTe which can lower the V_{oc}, but the reduction in lattice mismatch and interface states reduces the J_o and consequently a higher V_{oc} is obtained [22]. The effect of the inter-diffusion on device performance depends on the composition of the alloy formed during annealing. It was reported that for longer annealing durations, the S concentration in CdTe increases and reaches the solubility limit of S in CdTe [24].

In this paper we report on the study of inter-diffusion of S and Te across the CdTe/CdS interface using Auger electron spectroscopy (AES) technique. CdTe/CdS devices in the substrate configuration is ideal for the AES depth profile study since the junction is easily accessible than that

*Corresponding author.
E-mail address: jpe2005@gmail.com (J.P. Enríquez).

0927-0248/$ - see front matter © 2007 Elsevier B.V. All rights reserved.
doi:10.1016/j.solmat.2007.05.008

in the glass based superstrate configuration. The AES depth profile study of a substrate configuration CdTe/CdS device is discussed and the results are presented.

2. Experimental

The CdTe/CdS hetero junctions were prepared on stainless steel (SS) substrates (Goodfellow AISI 302) using the following procedure: CdTe film of approximately 8 μm thickness was deposited onto the substrate by CSS. The substrate and source temperatures were 570 and 670 °C, respectively [5,27]. The CdTe films were treated with a saturated solution of $CdCl_2$ in methanol, dried in air and annealed at 400 °C for 5 min in air. The CdTe/CdS junctions were developed by depositing approximately 0.2 μm CdS layer onto the CdTe substrates from a chemical bath containing 0.033 M cadmium acetate, 1 M-ammonium acetate, 28–30% ammonium hydroxide and 0.067 M thiourea. The deposition time was about 35 min. The bath was maintained at a constant temperature of 90 °C and continuously stirred during the deposition to ensure homogeneous distribution of the chemicals [28]. Finally the CdTe/CdS junctions were treated with a saturated solution of $CdCl_2$ in methanol and annealed for 20 min in air at different temperatures in the range 350−450 °C.

The cross-sectional composition profiles of the samples were obtained by Auger technique using a JAMP-7800 (JEOL) equipment, with a base pressure of 2×10^{-9} Torr. The parameters of the primary electron beam were: 3 keV of energy and 0.2 μA of current. The samples were inclined at 55° with respect to the normal of the surface. The AES depth profiles were obtained with a Ar^+ beam of 3 keV of energy and 20 mA of current. The atomic concentration of the elements is given by the following relationship [29]:

$$C_k = \frac{I_k/S_k}{\sum_i I_i/S_i}, \quad (1)$$

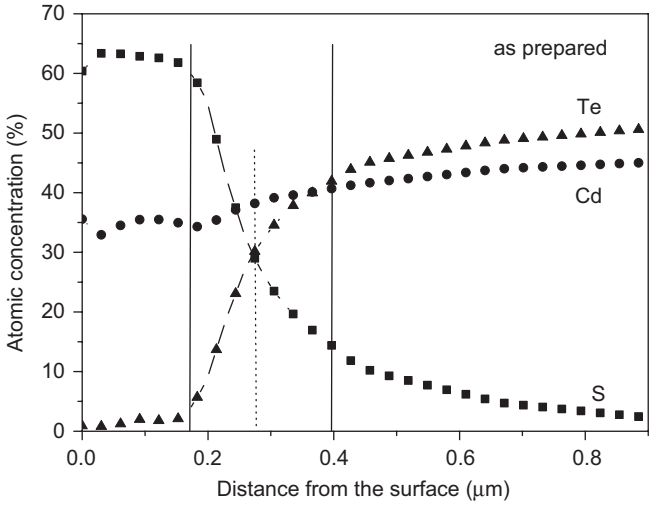

Fig. 1. Auger depth profile of the as prepared CdTe–CdS device.

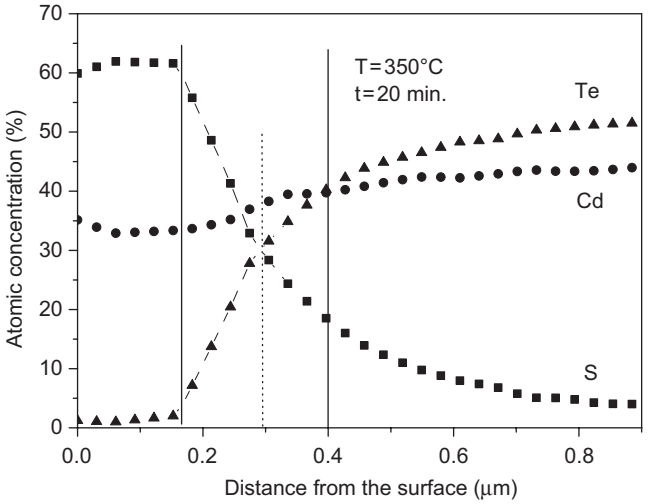

Fig. 2. Auger depth profile of the CdTe–CdS device annealed in dry air at 350 °C for 20 min.

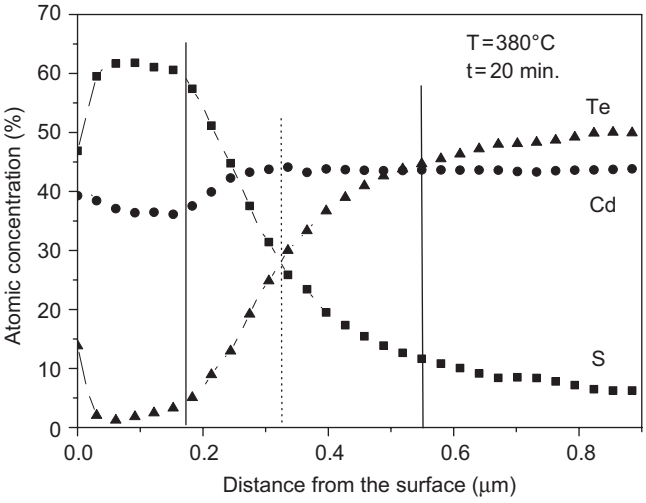

Fig. 3. Auger depth profile of the CdTe–CdS device annealed in dry air at 380 °C for 20 min.

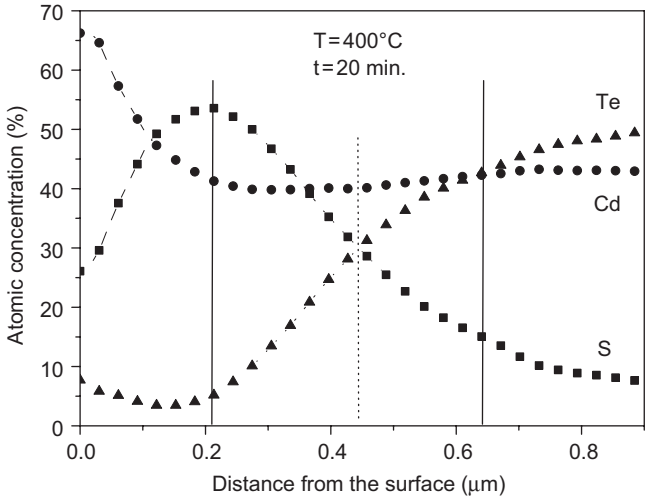

Fig. 4. Auger depth profile of the CdTe–CdS device annealed in dry air at 400 °C for 20 min.

where the sum is made for all the elements of the sample, C_k is the atomic concentration of element k, S_k is the Auger relative sensitivity factor of the element k and I_k is the peak-to-peak intensity in the Auger spectrum of element k. In the case of CdTe–CdS, the Auger relative sensitivity factors are $S_{Cd} = 1$, $S_{Te} = 0.7$ and $S_S = 0.8$ [29]. XRD patterns were recorded using Cu-Kα radiation of a Rigaku RAD-C diffractometer.

3. Results and discussion

3.1. AES analysis

In Figs. 1–4 the relative atomic concentration of Cd, Te and S across the CdTe–CdS interface of the as-deposited and annealed samples are presented. These figures demonstrates the variation in atomic concentrations with respect to distance from the device surface and the influence of annealing temperature on the inter-diffusion of S and Te. Fig. 1 is the Auger depth profile of the as-deposited CdTe–CdS device. The stiochiometric boundaries of the CdS and CdTe films are shown with solid vertical lines. The region between the two vertical lines is taken as the width of the interface. It can be seen that the diffusion of S into the CdTe is very significant compared to the diffusion of Te into the CdS. The presence of S in the CdTe region is due to the diffusion of S and not due to the penetration of CdS from the chemical bath through the intergrain space. If the latter was the case, there should have been more Cd at the stiochiometric boundary than that in the bulk of the CdTe. But from the figure, it can be seen that the Cd concentration is more or less constant at the boundary and in the bulk of the CdTe. The 0.24 μm width of the interface region suggest that in as-deposited devices, there is a significant intermixing between CdTe and CdS, which may be occurred during the deposition of CdS. Thus the CdTe–CdS interface of the as-deposited device is not abrupt. It should be noted from the figure that the thickness of the CdS region is about 0.18 μm. The dotted line at a depth of 0.27 μm below the surface where the atomic concentration of S and Te becomes equal is considered as the metallurgical junction separating the S and Te rich regions of the interface. The CdTe film is rich in Te which is expected for the p-type CdTe.

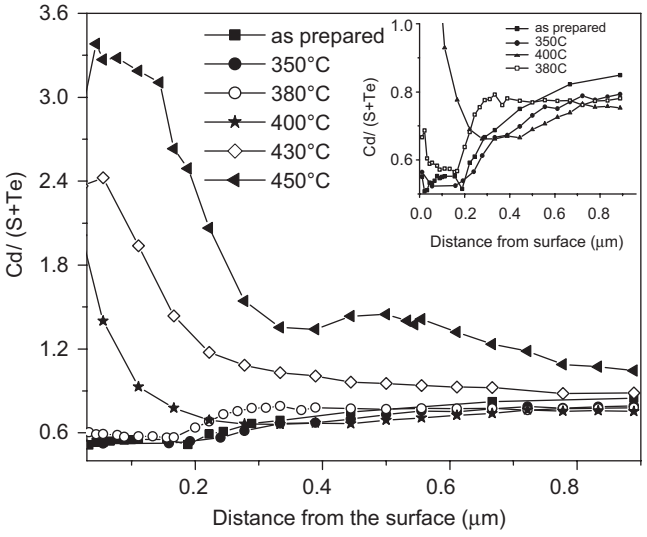

Fig. 5. Variation of the ratio Cd/(S + Te) with depth from the surface of the CdTe–CdS device. The inset is the expanded view of the profiles of four devices; as prepared (virgin) and annealed at 350, 380 and 400 °C.

Annealing at 350 °C (Fig. 2) does not make many changes in deposited device, except a small shift (0.02 μm) of the metallurgical junction towards the CdTe side and diffusion of more S. The Auger profile of the device annealed at 380 °C is shown in Fig. 3. The influence of annealing is noticeable; the width of the interface has increased to 0.36 μm, the metallurgical junction is further

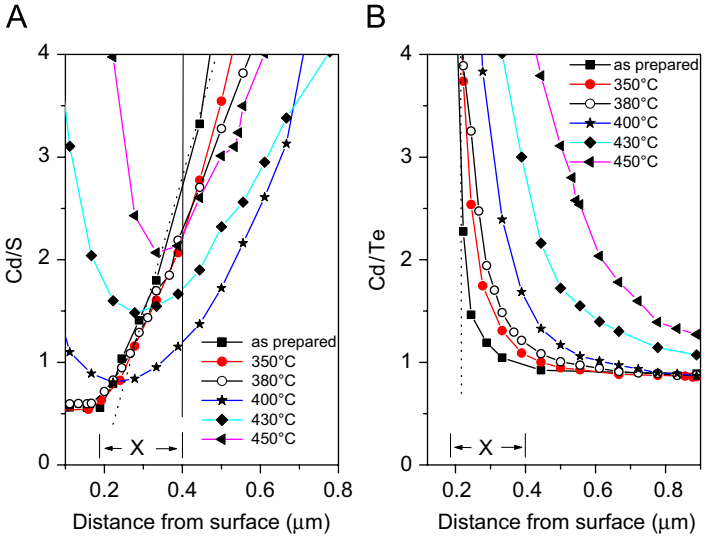

Fig. 6. Depth profiles showing the ratios (A) Cd/S and (B) Cd/Te across the CdTe–CdS interface and the bulk of the film for as prepared as well as the annealed devices.

shifted into the CdTe side and there is loss of S from the CdS surface and an increase in Te concentration at the surface. The increase in Te concentration at the surface is proportional to the loss of S, which suggests that the Te may be occupying the sites of S.

Annealing at 400 °C (Fig. 4) causes significant loss of S from the CdS surface leaving a Cd rich surface, the maximum concentration of S is at 0.2 μm from the surface, which was the stiochiometric boundary of the CdS. The interface width is increased to 0.48 μm and the metallurgical junction is moved to 0.44 μm. It can be seen that more Te is diffusing from CdTe into the interface and migrating to the CdS from the interface. It is interesting to note that in Figs. 1–3, the S and Te profiles are more or less symmetric in CdS, the interface and in CdTe indicating that both S and Te are occupying the sites left by each other in CdTe and CdS. But in the case of device annealed at 400 °C, the S and Te profiles are asymmetric in the CdS film indicating that the influx of Te is not sufficient to fill the sites of sublimated S. For annealing temperatures higher than 400 °C, we have observed complete depletion of S from the surface due to both diffusion and sublimation, indicating degradation of the CdTe–CdS hetero junction.

Fig. 5 shows the ratio of Cd to the anion (S + Te) in the CdS, interface, and CdTe regions of the hetero-structures annealed at different temperatures. A clear distinction between devices annealed below and above 400 °C can be observed. At temperatures above 400 °C the increase of this ratio in the CdS side suggests a deficiency of the anion (Te + S), due to diffusion of S into the CdTe layer, as well as sublimation from the CdS surface. As our as-deposited CdS films are rich in S (Fig. 1), the influx of Te during annealing might not be enough to occupy all the vacant S sites. In the similar fashion, the observed increase of the ratio in the interface region and the bulk of CdTe film after annealing at higher temperatures is expected as the diffusion of S from the already S depleted CdS side is much lower than the diffusion of Te from the CdTe side. The net effect is a decrease in the concentration of the anions.

The ratio Cd/(S + Te) for the devices annealed at temperatures below 400 °C is expanded and presented in the inset of Fig. 5. Though the variations between the curves are very small, a systematic change can be observed in the CdTe region. In the CdTe film, the ratio decreases as annealing temperature increases until 400 °C, which can be explained as follows: upon annealing, S is diffusing into the interface and to the CdTe film from the CdS at a rate faster than the diffusion of Te from the CdTe film towards the interface and to the CdS. Thus there is an accumulation of anions in the CdTe film causing the ratio to decrease. The annealing at 350 °C do not make any noticeable difference at the CdS side or at the interface, but after annealing at 380 °C, the ratio increases in the CdS and in the interface indicating the migration of S towards CdTe film.

Fig. 6 shows the variation of the Cd/S and Cd/Te ratios providing a more useful interpretation of the Figs. 1–4. The width of the interface in the case of the as-deposited device is marked as X in the figure. For the as-deposited device, the variation of the ratio Cd/Te with distance (Fig. 6A) shows an abrupt edge near the CdS interface (the tendency is shown with solid line), indicating that the amount of diffused Te in the CdS film is almost negligible. In the interface region, the Te concentration shows a gradient and at the stiochiometric interface (depth = 0.4 μm) of the CdTe, the Te concentration is slightly more than that of Cd which is typical for the p-CdTe. Fig. 6B, which is the variation of the Cd/S ratio with depth, shows that unlike the Cd/Te ratio, the as-deposited device shows a gradient indicating the presence of S in both the interface and the CdTe film. This asymmetry between the relative

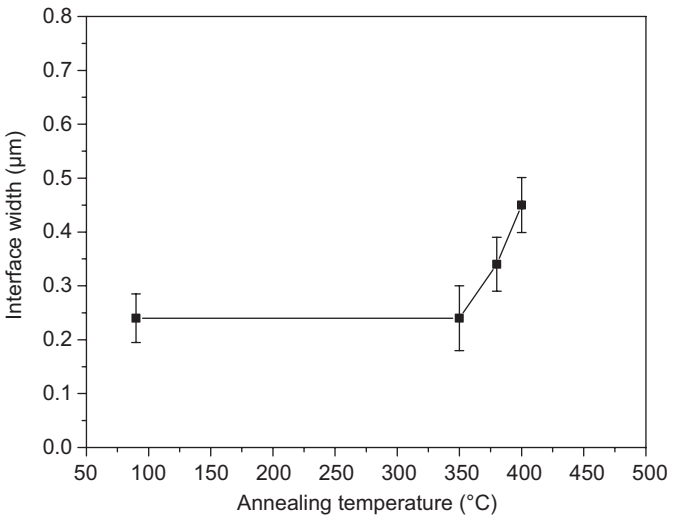

Fig. 7. Graph showing the dependence of interface width on annealing temperature of the CdTe–CdS device.

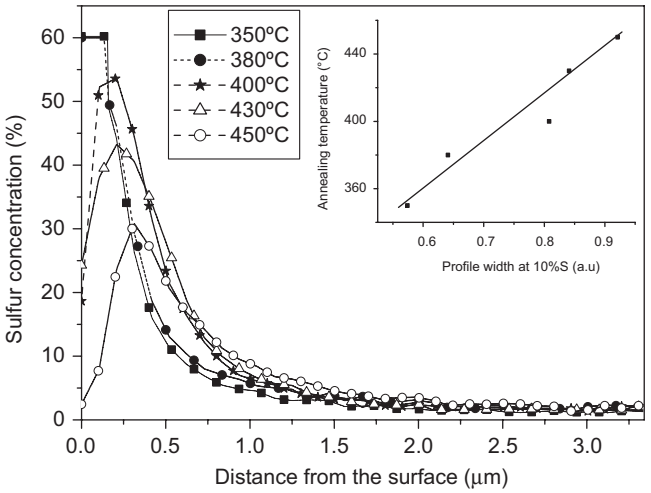

Fig. 8. The evolution of the S profile due to annealing. The inset shows the S profile width measured at 10% S concentration. The graph shows a linear relationship between the profile width and annealing temperature.

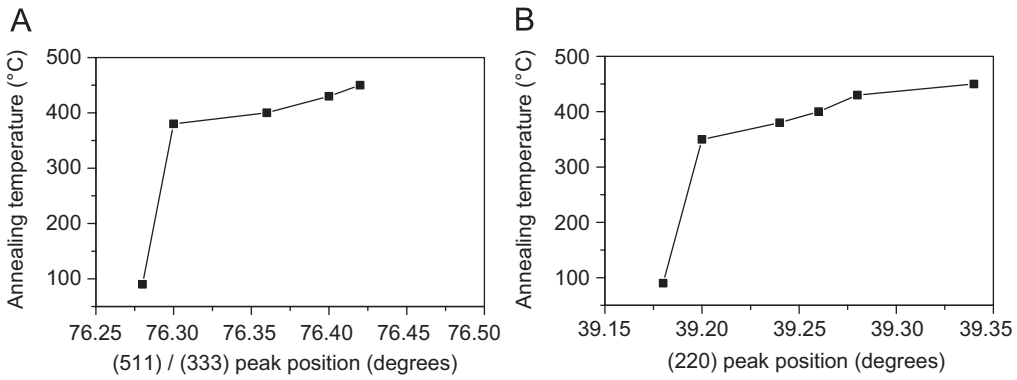

Fig. 9. Graphs showing the shift of the characteristic peaks of CdTe due to the formation of the alloy $CdTe_{1-x}S_x$. (A) (5 1 1)/(3 3 3) peak and (B) the (2 2 0) peak.

concentrations of S and Te is related with the different degree of diffusion of S and Te which is evident in Fig. 1 where the Te concentration is practically zero in the CdS layer. The significant differences observed in the Cd/S ratio for temperatures higher than 400 °C is in good agreement with the observation in Fig. 5.

Fig. 7 illustrates the variation of the interface width with annealing temperature. It can be seen that the interface width is affected only when annealing at temperatures higher than 350 °C. An increase in interface width can be interpreted as an increase in the region of the ternary compound $CdTe_xS_{1-x}$. The formation of the $CdTe_xS_{1-x}$ alloy due to inter-diffusion reduces the effect of lattice mismatch between CdTe and CdS and lowers the defect density at the interface.

Fig. 8 shows the concentration of S in the interface as well as in the bulk of the CdTe film for devices annealed at various temperatures. The profile broadening due to diffusion of S is observed at the interface (approximately 0.2−1 μm). In all the cases, a diffusion tail of nearly uniform concentration of S was formed in the bulk of the CdTe film. Thus the S profiles exhibit two features: a broad region corresponding to fast diffusion across the interface and into the CdTe film, and a slow diffusion which is independent of the annealing temperature. The width of the profile measured at 10% S concentration showed a linear relationship with the annealing temperature. The graph of profile width against annealing temperatures is shown in the inset of Fig. 8.

3.2. XRD results

The shift of the characteristic XRD peaks of the CdTe (2 2 0) and (5 1 1)/(3 3 3) are shown in Fig. 9. The shift of the peaks towards higher angles is indicative of the formation of the alloy $CdTe_xS_{1-x}$ [22,24]. The consistent shift of the peaks shows a significant degree of S diffusion with temperature. Such a systematic shift was not observed in the case of CdTe films treated with $CdCl_2$ and annealed at 350, 400 and 450 °C for 20 min (not shown). Thus, the observed shift in the case of CdTe–CdS device is due to the formation of the ternary alloy at the interface.

4. Conclusion

The extent of inter-diffusion of S and Te in a substrate configuration CdTe/CdS solar cell due to annealing is studied using AES depth profiling. The as-deposited device showed significant diffusion of S into the CdTe creating an interface region of approximately 0.2 μm width. The width of the interface region increases upon annealing. Annealing causes the inter-diffusion of S and Te occupying the sites of each other in CdS and CdTe, respectively. However, S diffuses faster than Te. The observed shift of the XRD peaks of the CdTe and CdS suggest the formation of a ternary compound at the interface.

Acknowledgments

The films and devices were prepared at CIE-UNAM. The CdTe program at CIE was supported by CONACYT project SEP-2004-C01-47587 and PAPIIT-UNAM projects IN115102 and ES-113707, respectively. J.P.E. acknowledges the support of the PROMEP through the project UPCHIS-PTC-006.

References

[1] M.P.R. Panicker, M. Knaster, F.A. Kroger, J. Electrochem. Soc. 125 (1978) 566.
[2] A.E. Rakhshani, Y. Makdisi, X. Mathew, N.R. Mathews, Phys. Stat. Sol. (A) 168 (1998) 177.
[3] X. Mathew, P.J. Sebastian, Sol. Energy Mater. Sol. Cells 59 (1999) 85.
[4] X. Mathew, P.J. Sebastian, A. Sanchez, J. Campos, Sol. Energy Mater. Sol. Cells 59 (1999) 99.
[5] G.P. Hernández, X. Mathew, J.P. Enríquez, B.E. Morales, M.M. Lira, J.A. Toledo, A.S. Juárez, J. Campos, J. Mater. Sci. 39 (2004) 1515.
[6] H.R. Moutinho, F.S. Hasoon, F. Abulfotuh, L.L. Kazmerski, J. Vac. Sci. Technol. A 13 (6) (1995) 2877.
[7] P.D. Paulson, X. Mathew, Sol. Energy Mater. Sol. Cells 82 (2004) 279.
[8] X. Mathew, J. Phys. D 33 (2000) 1565.
[9] X. Mathew, J.R. Arizmendi, J. Campose, P.J. Sebastian, N.R. Mathews, C.R. Jimenez, M.G. Jimenez, R. Silva-Gonzalez, M.E. Hernandez-Torres, R. Dhere, Sol. Energy Mater. Sol. Cells 70 (2001) 379.
[10] X. Mathew, J. Mater. Sci. Lett. 21 (2002) 529.
[11] X. Mathew, Semicond. Sci. Technol. 18 (2003) 1.

[12] J.P. Enríquez, X. Mathew, J. Cryst. Growth 259 (2003) 215.
[13] X. Mathew, G.W. Thompson, V.P. Singh, J.C. McClure, S. Velumani, N.R. Mathews, P.J. Sebastian, Sol. Energy Mater. Sol. Cells 76 (2003) 293.
[14] B.E. McCandless, R.W. Birkmire, Sol. Cells 31 (1991) 527.
[15] A.N. Tiwari, A. Romeo, D. Baetzner, H. Zogg, Prog. Photovolt. 9 (2001) 211.
[16] L.A. Kosyachenko, X. Mathew, V.V. Motushchuk, V.M. Sklyarchuk, Sol. Energy 80 (2006) 148.
[17] X. Mathew, G.P. Hernández, U. Pal, C. Magaña, D.R. Acosta, R. Guardian, J.A. Toledo, G.C. Puente, J.A.C. Carvayar, Sol. Energy Mater. Sol. Cells 82 (2004) 307.
[18] X. Mathew, J.P. Enriquez, A.N. Tiwari, A. Romeo, Sol. Energy 77 (2004) 831.
[19] L.A. Kosyachenko, X. Mathew, V.V. Motushchuk, V.M. Sclyarchuk, Semiconductors 39 (2005) 539 (Translated from Fizika i Tekhnika Poluprovodnikov, vol. 39, No. 5, 2005, pp. 569–572).
[20] D.L. Linam, V.P. Singh, J.C. McClure, G.B. Lush, X. Mathew, P.J. Sebastian, Sol. Energy Mater. Sol. Cells 70 (2001) 335.
[21] N. Romeo, A. Bosio, R. Tedeschi, A. Romeo, V. Canevari, Sol. Energy Mater. Sol. Cells 58 (1999) 209.
[22] B.E. McCandless, I. Youm, R.W. Birkmire, Prog. Photovolt. 7 (1999) 21.
[23] J. Britt, C. Ferekides, Appl. Phys. Lett. 62 (1993) 2851.
[24] B.E. McCandless, L.V. Moulton, R.W. Birkmire, Prog. Photovolt. 5 (1997) 249.
[25] D.H. Levi, H.R. Mountinho, F.A. Hasoon, B.M. Keyes, R.K. Ahrenkiel, M. Al-Jassim, L. Kazmerski, R.W. Birkmire, in: Proceedings of the First WCPEC, Hawaii, 1994, p. 127.
[26] D.M. Oman, K.M. Dugan, J.L. Killian, Appl. Phys. Lett. 67 (1995) 1896.
[27] G.P. Hernandez, A.S. Juarez, M.C. Resendiz, X. Mathew, Sol. Energy Mater. Sol. Cells 90 (2006) 2289.
[28] J.P. Enríquez, X. Mathew, Sol. Energy Mater. Sol. Cells 76 (2003) 313.
[29] L.E. Davis, N.C. MacDonald, P.W. Palmberg, G.E. Riach, R.E. Weber, Handbook of Auger Electron Spectroscopy, Perkin-Elmer, Eden Prairie, 1978.